INVESTIGATING THE UNEXPECTED YOUTH OF MERCURY'S PYROCLASTIC DEPOSITS. L. M. Jozwiak[1], C. M. Wagoner[1], N. R. Izenberg[1], [1]Planetary Exploration Group, Johns Hopkins University Applied Physics Laboratory, Laurel, MD, USA. (Corresponding author: lauren.jozwiak@jhuapl.edu).

Introduction: The MErcury Surface, Space ENvironment, GEochemistry, and Ranging (MESSENGER) mission [1] revealed evidence for explosive volcanism on Mercury [e.g. 2]. Throughout the course of the mission, several researchers mapped increasing numbers of features indicative of explosive volcanic activity [3-6], resulting in a final catalog identifying 104 pyroclastic vents [7]. These vents are distributed across the surface of the planet [6, 7], and unlike lunar pyroclastic deposits [e.g. 8], Mercury's pyroclastic deposits are not closely associated with the edges of impact basins, and appear to be anti-correlated with the locations of smooth volcanic plains [7].

The geologic history of Mercury has been interpreted to fall into two distinct periods: an early history that was dominated by the successive emplacement of generations of effusive volcanic plains [9], later followed by a protracted period of cooling and contraction dominated by the formation of lobate scarps and other compressional tectonic features [10, 11]. Crater size-frequency distribution studies of both smooth plains deposits and lobate scarps support this bimodal geologic history. Effusive volcanic plains appear to have ceased formation ~3.5 Ga [12] during the early Calorian period. In contrast, lobate scarp formation and activation appears to have begun in the mid-Calorian period and extended through the remainder of Mercury's history [11, 13].

We examine the relative ages of the pyroclastic vents to investigate how they fit into the overall thermal and geologic history of Mercury.

Stratigraphic Method: Unlike many planetary surfaces, crater size frequency distribution analysis cannot be used to determine the model age of pyroclastic deposits because of the difficulty in determining superposition relationships between craters on the deposit and under the deposit, and uncertainties in how the fine-grained pyroclastic material retains craters [14]. Instead, previous work [5, 7] utilized a stratigraphic method for establishing a range of ages for pyroclastic vents. Because the majority (82%) of vents are located inside impact craters [7], the stratigraphic age of the host crater can be used to place an upper bound on the age of the interior vent. Using the updated crater classification scheme of [15], we previously determined that the majority of vents (70%) are located in Tolstojian and Calorian period craters [7]. This was an expected result, given that the majority of impact craters on Mercury are associated with these periods [15]. However, a surprising result from this analysis was the observation of 10 vents inside Mansurian period craters, and 1 vent inside a crater associated with the Mansurian/Kuiperian boundary [7]. The Mansurian period began ~1.7 Ga, and the Kuiperian as recently as ~280 Ma; thus suggesting explosive volcanism may have occurred in Mercury's recent geologic history.

Despite these intriguing results, the stratigraphic method has severe limitations, particularly in investigating the ages of vents not associated with craters. The method additionally biases results towards older ages, as it cannot determine how long vent formation occurred after crater formation. In order to examine these questions, we have devised a new relative system of vent dating, which relies upon the morphologic degradation state of the vent, combined with the spectral characteristics of the associated pyroclastic deposit.

Vent Degradation: Mercury's pyroclastic vents display a wide range of morphologies, and apparent levels of degradation [4-7]. For example, Fig. 1 displays two of the earliest observed vents, (A) Nathair facula (previously NE Rachmaninoff) (35.8° N, 63.8° E), and (B) an unnamed vent in the crater Glinka (14.9° N, 112.4° W). Differences in the apparent freshness of morphology can clearly be observed in the wall texture, the presence/absence of layering, and the floor texture. Building upon these qualitative observations, we developed a morphologic degradation classification system for the volcanic vents on Mercury. Our analysis used the Mercury Dual Imaging System (MDIS) monochrome global mosaic for context, and all available high-resolution MDIS Wide and Narrow Angle Camera (WAC and NAC) images for each vent to classify the vents into three categories [16]: (1) oldest/most degraded, (2) moderate degradation, and (3) youngest/least degraded. The process of classification, along with details of the geomorphologic markers are provided in Wagoner and Jozwiak (abstract #1437, this volume) [16]. The degradation method identified 10 Class 3 (young) vents, 68 Class 2 vents, and 39 Class 1 (old) vents.

While this classification system is self-consistent, it is hindered by image availability, and therefore is conservatively biased towards older morphologies. In order to establish an independent assessment of the degradation classification system, we also investigated deposit reflectance.

Pyroclastic Deposit Reflectance: Early analysis [5] of the Mercury Atmospheric and Surface Composition Spectrograph – Visible and Infrared Spectrometer (MASCS-VIRS) [17] data identified two principle spectral characteristics of pyroclastic deposits: depth of UV absorptions, and reflectance at 700nm, and used these parameters to categorize vents into 4 spectral classes. It has been hypothesized [5] that the variations in reflectance at 700 nm are due to variations in space weathering, and therefore, deposit age. Previous analysis [18] has shown that host crater stratigraphic age is a poor predictor of overall deposit reflectance or other spectral properties. This is unsurprising, given that a vent can be significantly younger than the host crater, something observed frequently in our degradation classification.

In order to investigate the viability of our degradation classification, we select several vents from each of the degradation classes, and plot the same parameters (Fig. 2). We observe a trend of increasing deposit reflectance with decreasing vent age. The single exception is the Class 1 vent located at (33.4° N, 88.1° E), which appears anomalously high reflectance for its degradation level; however, this vent is located well within the bright crater ray system of the crater Fonteyn, and this signal is likely contributing to the perceived brightness of the deposit.

Results and Ongoing Work: After previously establishing that pyroclastic vent formation may have occurred in recently in Mercury's history [7], we have now established a new method to investigate the temporal distribution of explosive volcanism throughout that history. Through use of a relative degradation classification system, we can investigate vent age independently of host crater age. Our analyses have shown that our degradation classification system is consistent with trends in the pyroclastic deposit reflectance at 700 nm, a parameter previously hypothesized to be related to vent age via space weathering. We are now working to expand the spectral analysis to include all of the vents in the catalog, and to remove regional brightness trends (such as crater rays) by ratioing deposit spectra to nearby background material. We are also exploring any trends in spatial distribution related to vent age and deposit reflectance, as well as, possible trends relating to the UV parameter.

All of our analyses continue to support the conclusion that not only was explosive volcanism occurring in Mercury's recent geologic past, but the majority of explosive volcanic vents on Mercury may have have formed well after the cessation of effusive volcanism. This has significant implications for thermal models of Mercury's evolution [19, 20, 21], which must now provide mechanisms for melt production and mama ascent well past what was thought possible.

References: [1] Solomon, S. C., et al. [2007] *Space Sci. Rev. 131*, 3-39. [2] Head, J. W., et al. [2008] *Science 321*, 69-72. [3] Kerber, L., et al. [2009] *EPSL 285*, 263-271. [4] Kerber, L., et al. [2011] *PSS 59*, 1895-1909. [5] Goudge, T. A., et al. [2014] *JGR Planets 119*, 635-658. [6] Thomas, R. J., et al. [2014] *JGR Planets 119*, 2239-2254. [7] Jozwiak, L. M., et al. [2018] *Icarus 302*, 191-212. [8] Gaddis, L. R., et al. [2003] *Icarus 161*, 262-280. [9] Denevi, B. W., et al. [2013] *JGR Planets 118*, 891-907. [10] Byrne, P. K., et al. [2014] *Nature Geosci. 7*, 301-307. [11] Crane, K. T., and Klimczak, C. [2017] *GRL 44*, 3082-3089. [12] Byrne, P. K., et al., [2016] *GRL 43*, 7408-7416. [13] Banks, M. E., et al. [2017] *JGR Planets 122*, 1010-1020. [14] Luchitta, B. K., and Schmitt, H. H. [1974] *LPS V*, 223-234. [15] Kinczyk, M. J., et al. [2016] *LPSC 47*, Abstr. #1573. [16] Wagoner, C. M. and Jozwiak, L. M. (2020) *LPSC LI*, Abstract #1437. [17] McClintock, W. E., and Lankton, M. R. [2007] *Space Sci. Rev. 131*, 481-521. [18] Jozwiak, L. M. et al. (2018) *LPSC XLIX*, Abstract #2324. [19] Michel, N. C. et al. (2013) *JGR Planets, 118*, 1033-1044. [20] Tosi, N. M., et al. (2013) *JGR Planets, 118*, 2474-2487. [21] Evans, A. J. et al. (2015) *LPSC XLVI*, Abstract #2414.

Figures:

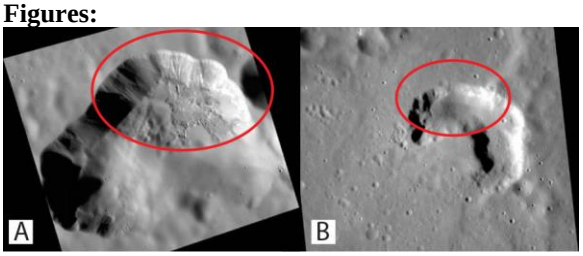

Figure 1: Geomorphologic comparison of the vents (A) Nathair facula (formerly NE Rachmaninoff) and (B) Glinka. The floor of Nathair facula displays fresh textured morphology, and visible wall layering, while Glinka has degraded featureless walls, and a muted floor.

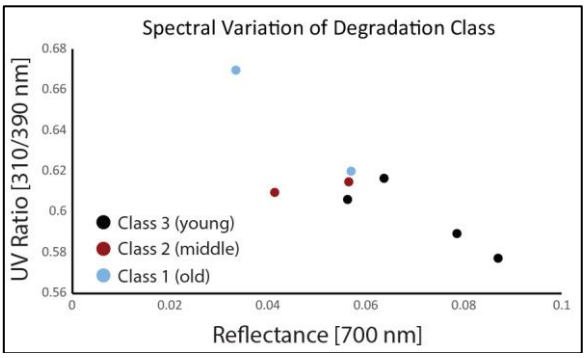

Figure 2: Vent spectral parameters as a function of geomorphologic degradation class. Deposit reflectance increases with decreasing degradation. This is consistent with reflectance at 700 nm being a proxy for vent age.